Effects of hypothetical complex mass-density distributions on geoidal height

Robert Kingdon, Petr Vaníček, Marcelo Santos
Department of Geodesy and Geomatics Engineering,
University of New Brunswick, P.O. Box 4400, Fredericton, NB, Canada, E3B 1L6

Abstract. Geoid computation according to the Stokes-Helmert scheme requires accurate modelling of the variations of mass-density within topography. Current topographical models consider only horizontal variations, although in reality density varies three-dimensionally. The lack of knowledge of regional three-dimensional density distributions prevents evaluation from real data. In light of this deficiency, we attempt to at least estimate the order of magnitude of the error in geoidal heights caused by neglecting the depth variations by calculating, for artificial but realistic mass-density distributions, the difference between results from 2D and 3D models.
Our previous work has shown that for simulations involving simple mass-density distributions in the form of planes, discs or wedges, the effect of mass-density variation unaccounted for in 2D models can reach centimeter-level magnitude in areas of high elevation, or where large mass-density contrasts exist. However, real mass-density distributions are still more complicated than those we have modeled so far, and involve multiple structures. To expand on our previous work, we now present results for effects on geoidal height of mass-density structures involving multiple shapes and interfaces. We form a more complex structure by creating an array of discs. By this simulation we show that even in the presence of complex density distributions, vertical variations of topographical density will have only a centimeter level effect on the geoid.

Keywords. Geoid, topographical density, density model, direct topographic effect, primary indirect topographic effect.

1 Introduction

The Stokes-Helmert method of geoid modeling requires determination of effects of all topographical masses in order to convert gravity anomalies to the Helmert space, and to convert the Helmert co-geoid from the Helmert space back to the real space. These calculations have traditionally used a constant value of topographical density (e.g. Vaníček and Kleusberg 1987), but numerous investigations have shown that to obtain a precise geoid the effects of density variations within topography must also be calculated (e.g. Martinec 1993; Pagiatakis et al. 1999; Huang et al. 2001). These efforts have almost exclusively focused on horizontal density variations. Since the actual topographical density varies with depth, two dimensional topographical density models (2DTDMs) currently in use cannot accurately model the real density distribution. However, three dimensional topographical density models (3DTDMs) are not practical for real world calculations since the 3D density structure of the topography is known to a reasonably high resolution only over small areas (e.g. for local geophysical studies or prospecting), or to very coarse resolutions over large areas (e.g. the CRUST 2.0 model developed by Bassin et al. 2000). Unfortunately, it is not yet possible to construct a 3DTDM to a high enough resolution and over a large enough area to be good enough for geoid modeling (Kuhn 2003).
Notwithstanding the current impossibility of applying a 3DTDM based on real data, we attempt to determine the potential shortcomings of 2DTDMs and ultimately to delineate situations where those shortcomings will lead to significant errors in geoid determinations. Kingdon et al. (2009) recently showed that in the presence of single 3D bodies of anomalous topographical density, using only a 2DTDM might introduce errors of up to several centimeters in areas of high topography. In reality, topography does not consist of single bodies of anomalous density, but is a much more complex arrangement of bodies of varying densities. In this effort, we try to discover whether in extreme cases adjacent density bodies can either mitigate or reinforce each other's effects on the geoid. If even in this extreme case effects of adjacent masses cancel each other out, then we can suppose that 3DTDMs are rarely needed in real world applications. However, if the effects are

significant then more work is necessary to define situations where 3DTDMs are needed. The investigation is done within the framework of the Stokes-Helmert scheme of geoid modeling, following the methodology discussed in Section 2. Section 3 will show and discuss our results using this methodology, and finally we will present the conclusions derived from our results and make recommendations for future work in Section 4.

2 Methodology

2.1 3D density modeling in the Stokes-Helmert context

The Stokes-Helmert method of geoid computation requires a model of topographical density both for calculating the transformation of gravity anomalies to the Helmert space (called the Direct Topographical Effect or DTE), and for calculating the transformation of the Helmert co-geoid back to the real space (the Primary Indirect Topographical Effect or PITE) after the Stokes integration (Martinec et al., 1994a, 1994b). Existing models normally consider topography of constant density (usually 2670 kg m^{-3}). For our modeling, we will be considering the variation of topographical density from the average values in a three dimensional sense. We label this anomalous topographical density $\delta\rho$.

Each of the transformations required in the Stokes-Helmert method comprises an evaluation of the difference between the effect of real and condensed anomalous topographical density at the location of each gravity anomaly. Here, we follow the same approach outlined in Kingdon et al. (2009), which is a generalization of the approach given by Martinec (1998). The DTE on gravity is calculated by the integral formula:

$$\varepsilon^{\delta\rho}_{DTE}(r,\Omega) = \iint_{\Omega'} \frac{\partial}{\partial r}\left[\int_{r'=r_g(\Omega')}^{r_t(\Omega')} \delta\rho(r',\Omega')K(r,\Omega;r',\Omega')r'^2 dr' - \delta\sigma(\Omega')K(r,\Omega;r_g(\Omega'),\Omega')r_g(\Omega')\right] d\Omega' , \quad (1)$$

where $\varepsilon^{\delta\rho}_{DTE}$ is the DTE on gravity at a point given by its geocentric radius r and a geocentric direction Ω, representing its geocentric latitude and longitude. $\delta\rho$ is the anomalous density at an integration point with coordinates r', Ω', given by a 3DTDM. $r_t(\Omega')$ and $r_g(\Omega')$ are the surface of the topography and the geoid, respectively. The function $K(r,\Omega;r',\Omega')$ is the Newton kernel, equal to the inverse distance between the computation and integration points.

The PITE on gravitational potential, $\varepsilon^{\delta\rho}_{PITE}(R,\Omega)$, is calculated by the formula:

$$\varepsilon^{\delta\rho}_{PITE}(r_g(\Omega),\Omega) = \iint_{\Omega'}\left[\int_{r'=r_g(\Omega')}^{r_t(\Omega')} \delta\rho(r',\Omega')K(r,\Omega;r',\Omega')r'^2 dr' - \delta\sigma(\Omega')K(r,\Omega;r_g(\Omega'),\Omega')r_g^2(\Omega')\right] d\Omega' . \quad (2)$$

Notice that the DTE is evaluated at the topographical surface, since this transformation is applied to gravity anomalies at the topographical surface. The PITE is evaluated at the geoid surface, which we approximate for the evaluation of the Newton kernels as a sphere of radius R = 6 371 008.144 m, the mean radius of the Earth. Furthermore, the condensation density referred to in these formulas is calculated for a 3DTDM according to:

$$\delta\sigma(\Omega) = \frac{1}{R^2}\int_{r'=r_g(\Omega)}^{r_t(\Omega)} r'^2\,\delta\rho(r',\Omega)\,dr' . \quad (3)$$

For our investigation, we convert the effects in Eqs. (1) and (2) into effects on geoidal heights. In the case of the DTE, the effect can be computed to a suitable precision by applying Stokes integration to the DTE on gravity:

$$\delta N^{\delta\rho}_{DTE}(\Omega) \doteq \frac{1}{4\pi\gamma(\Omega)}\iint_{\Omega'} S(\psi[\Omega,\Omega'])\varepsilon^{\delta\rho}_{DTE}(\Omega')\,d\Omega' , \quad (4)$$

where $\delta N^{\delta\rho}_{DTE}$ is the DTE on geoidal height, $\gamma(\Omega)$ is the normal gravity, and $S(\psi[\Omega,\Omega'])$ is the Stokes kernel.

In the case of the PITE, the effect on geoidal height is found by applying Bruns's formula:

$$\delta N^{\delta\rho}_{PITE}(\Omega) = \frac{\varepsilon^{\delta\rho}_{PITE}(\Omega)}{\gamma(\Omega)} . \quad (5)$$

These effects on geoidal height allow us to compare the effects of masses to some meaningful tolerance to determine whether they are significant. In this case, where we are looking for a 1 cm geoid, we will have to consider any effect over 0.5 cm to be significant.

2.2 Numerical considerations

The Newton kernel and its integrals and derivatives in Eqs. (1) and (2) can be computed numerically in various ways. For our computation, we use the prismoidal method (Nagy et al. 2000, 2002) for integration over the neighbourhood of the computation point, and 2D numerical integration (e.g Martinec 1998) farther from the computation point.

In the prismoidal method, the anomalous topographical masses coming from the 3DTDM are divided into blocks, and the integral of the Newton kernel in planar coordinates over each block is calculated analytically. This formulation captures very well the behavior of the Newton kernel near to the computation point, and in that region is superior to 2D numerical integration, even though the 2D integration normally uses the more accurate spherical expression of the Newton kernel. The prismoidal formula is also faster than other analytical methods such as the polyhedral method. It is also faster in this particular case than the tesseroidal method, which must use a Taylor series expansion to greater than degree 2 to be sufficiently accurate very near to the computation point.

Comparison of the planar Newton kernels used in the prismoidal approach and the spherical Newton kernels shows that the kernels used to evaluate the DTE are more than 1 % different beyond 5 arc-minutes from the computation point, and that those used to evaluate the PITE are more that 1 % different beyond 15 º from the computation point. Fortunately, beyond these radii we can achieve sufficient accuracy using 2D numerical integration so these differences are moot. The 2D integration employs the radial integrals of the Newton kernel developed by Martinec (1998) to perform the radial integration of the Newton kernel over any given topographical column, thus evaluating the radial integral analytically. The horizontal integration is performed by dividing the integration area into cells, and summing the products of the values of the integrands in Eqs. (1) and (2) at the centers and the areas of each cell. This is faster than using the prismoidal formula, and provides sufficient accuracies for our preliminary investigation. The 2D horizontal integration is suitable beyond about 5 arc-minutes of the computation point for the DTE, and beyond 1 º of the computation point for the PITE. For our evaluations of the PITE, we use the prismoidal formula within 5 º of the computation point, to take greater advantage of its superior accuracy near the computation point.

A problem remaining in all of our investigations is discretization error. With both of the methods we have chosen above, the actual mass distribution of the topography is represented as a series of rectangular prisms. Even with other methods, it is discretized, whether by division into tesseroids or into polyhedrons. Some methods may minimize the discretization error, but it always remains, and it is very difficult to quantify since its behavior changes for different mass distributions. We can mitigate discretization error by using a smaller cell or prism size in our integration procedures; by extensive testing we have found that for the discs used here a resolution of 1 arc-second x 1 arc-second is sufficient. However, for small discs a higher resolution would be necessary, and for larger discs a lower resolution would suffice.

For the purposes of this investigation, we have tested our numerical integration against the single case of a disc, using analytical formulas for the DTE on gravity and PITE on gravity potential at the center of the disc. This is the point where the PITE caused by the disc is greatest, and a point where the DTE is very large. In this test, we find errors of up to 18 % in the numerical integration for the DTE and 5 % for the PITE in extreme cases, but normally less than 5 % for the DTE and 1 % for the PITE. The larger errors occur when the mass is very small, and consequently do not indicate a large magnitude of overall error. We consider such errors admissible for this exercise, as we only seek the order of magnitude of differences between results from 3DTDMs and 2DTDMs.

2.3 Proposed tests

Our question is: can the effect on geoidal height of a density body that, individually has a significant effect, be mitigated or enhanced by the presence of adjacent density contrast bodies? To investigate this, we take two extreme cases, each involving an array of anomalous masses. In case A, we choose masses that individually are known to have a particularly large DTE, and investigate the effect of the conglomerate of these masses on geoidal height. In case B, we choose masses known to have a large PITE. These two represent extreme cases, and will show in whether adjacent masses diminish each other's effect.

In both cases A and B, we use an array of vertical cylinders as our density model. These are considered as anomalous masses, and are assigned alternating density contrasts of positive or negative 600 kg m^{-3}. The anomalous density outside the cylinders is zero.

Our past work on individual mass bodies has shown us that both the DTE and PITE are greatest when:

1. the topography involved is thick,
2. anomalous density is distributed away from the geoid, and
3. there is a large density contrast.

Regarding the horizontal size of the bodies, for the PITE the larger the body the greater its effect will be, although the rate at which the effect increases becomes lower for wider bodies. For the DTE, by contrast, there is a range of horizontal sizes around 3300 m where the effect is normally the greatest. Thus, we use 3300 m as the disc diameter for case A. For case B we use 110 000 m as the disc diameter, beyond which the PITE does not increase very rapidly. In order to accommodate items 1 and 2 in the list above, we choose flat topography 2000 m thick, and use discs extending from the surface of the topography to 500 m depth.

We calculate results over a 1 º by 1º area for our case A simulation, and a 2 º by 2 º area for our case B simulation, both described in Section 3 below. We use a radius of 2 º for Stokes integration, and so our array of cylinders in case A extended over a 5 º by 5 º area to capture most of their effect.

3 Results

3.1 Case A

The DTE on gravity for case A, as described in section 2.3, is given in Fig. 3.1.

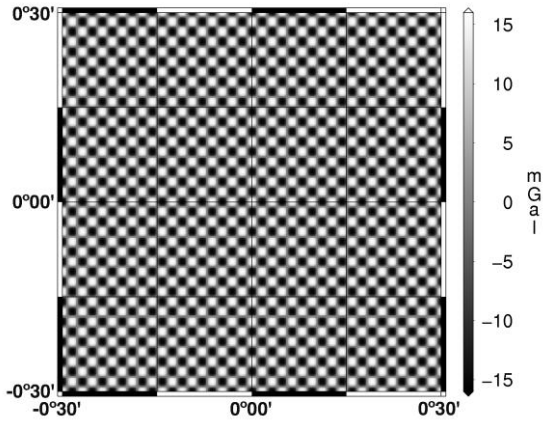

Fig. 3.1. DTE on gravity for case A.

The adjacent masses do not significantly diminish the DTE, which reaches +/- 16 mGal. This is not surprising, since the derivative of the Newton kernel, used to calculate these effects, decreases very rapidly with distance from the source masses. However, we are ultimately interested in the DTE on geoidal height, resulting from the Stokes integration (Eq. (4)), and given in Fig. 3.2.

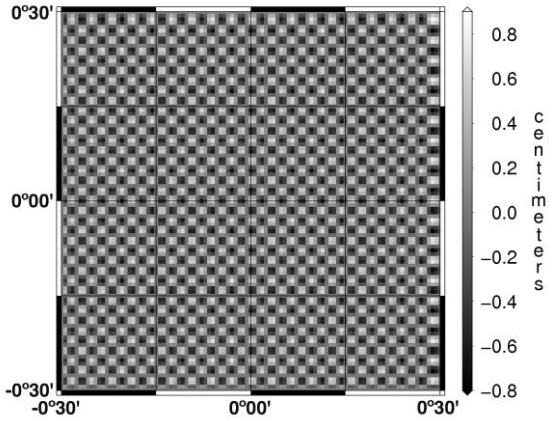

Fig. 3.2. DTE on geoidal height for case A.

We see that under the smoothing influence of the Stokes kernel, the adjacent masses largely attenuate each other's contributions to the DTE on the geoidal height, which reach about +/- 0.85 cm. This may not be the case for wider density anomalies, and it remains to find the maximum effect that masses can have in a simulation like our own.

3.2 Case B

The PITE on gravity for case B, as described in section 2.3, is given in Fig. 3.3.

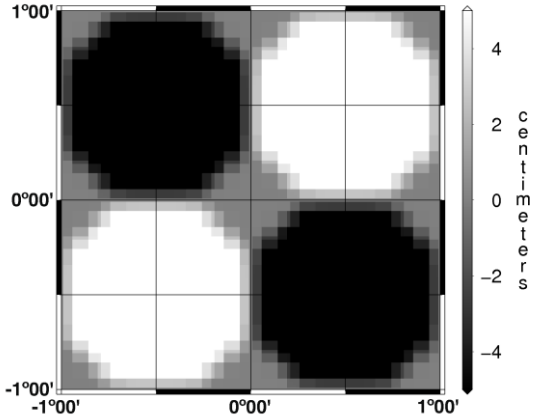

Fig. 3.3. PITE on geoidal height for case B.

We see that for such large cylinders, the effect of adjacent cylinders of opposite mass is minimal. Here the effects reach +/- 5 cm, but for larger discs

the magnitude would be greater and the attenuation even less significant. It is thus likely that effects on gravity will only increase for wider cylinders.

4 Conclusions

The DTE on gravity and the PITE on geoidal height for the anomalous masses in our simulations are neither significantly diminished, nor significantly increased by the presence of adjacent anomalous masses, even when there is an extreme density contrast. The PITE still reaches about 5 cm, and the DTE reaches about 16 mGal. This demonstrates that the error in the PITE resulting from using a 2DTDM will not be diminished significantly by adjacent mass anomalies.

The DTE on geoidal height is significantly diminished by the presence of adjacent masses, though it still approaches 1 cm level. However, this is entirely a result of Stokes integration, which was not considered in the development of our extreme case scenarios. With this in mind, larger bodies of anomalous density that still have a significant impact on the DTE on gravity may produce significantly larger effects on geoidal heights. This is now a new area for further investigation.

It is clear from our results that even in complex distributions, 3DTDMs may be needed to achieve a one centimeter geoid. The next step is to further clarify what types of density anomalies can have a significant influence on the geoidal height. For example, what is the size of anomalous density bodies in arrays of various parameters that leads to serious shortcomings in 2DTDMs? Or, can we say based on the spatial frequency of the mass distribution whether we expect the effects of masses to cancel each other out?

References

Bassin, C., G. Laske, and G. Masters (2000). The Current Limits of Resolution for Surface Wave Tomography in North America. *EOS Trans AGU*, 81, F897.

Huang, J., P. Vaníček, S. Pagiatakis and W. Brink (2001). Effect of topographical density variation on geoid in the Canadian Rocky Mountains. *Journal of Geodesy*, 74, pp. 805–815.

Kingdon, R., P. Vaníček and M. Santos (2009). First results and testing of a forward modelling approach for estimation of 3D density effects on geoidal heights. *Canadian Journal of Earth Sciences*, Vol 46, No. 8, pp. 571–585, DOI: 10.1139/E09-018.

Kuhn, M. (2003). Geoid determination with density hypotheses from isostatic models and geological information. *Journal of Geodesy*, 77, pp. 50–65.

Martinec, Z. (1993). Effect of lateral density variations of topographical masses in improving geoid model accuracy over Canada. Contract report for Geodetic Survey of Canada, Ottawa.

Martinec, Z. and P. Vaníček (1994a). Direct topographical effect of Helmert's condensation for a spherical approximation of the geoid. *Manuscripta Geodaetica*, 19, pp. 257–268.

Martinec, Z. and P. Vaníček (1994b). The indirect effect of topography in the Stokes-Helmert technique for a spherical approximation of the geoid. *Manuscripta Geodaetica*, 19, pp. 213–219.

Martinec, Z. (1998). *Boundary Value Problems for Gravimetric Determination of a Precise Geoid (Lecture Notes in Earth Sciences)*. Springer-Verlag, New York.

Nagy D., G. Papp and J. Benedek (2000). The gravitational potential and its derivatives for the prism. *Journal of Geodesy*, 74, pp. 552–560, DOI: 10.1007/s001900000116.

Nagy D., G. Papp and J. Benedek (2002). Corrections to "The gravi- tational potential and its derivatives for the prism". *Journal of Geodesy*, 76, p. 475, DOI: 10.1007/s00190-002-0264-7.

Pagiatakis, S., D. Fraser, K. McEwen, A. Goodacre and M. Véronneau (1999). Topographic mass density and gravimetric geoid modelling. *Bollettino di Geofisica Teorica e Applicata*, 40, pp. 189–194.

Vaníček, P. and A. Kleusberg (1987). The Canadian geoid – stokesian approach. *Manuscripta Geodaetica*, 12, pp. 86–98.